

Diterpenoids from aerial parts of *Flickingeria fimbriata* and their nuclear factor-kappaB inhibitory activities

Hang Li^a, Jing-jun Zhao^a, Jin-long Chen^b, Long-ping Zhu^{a,c}, Dong-mei Wang^{a,c}, Lin Jiang^{a,c}, De-po Yang^{a,c,*}, Zhi-min Zhao^{a,c,*}

^aSchool of Pharmaceutical Sciences, Sun Yat-sen University, Guangzhou, Guangdong 510006, China

^bSchool of Environmental and Chemical Engineering, Nanchang University, Nanchang, Jiangxi 330031, China

^cGuangdong Technology Research Center for Advanced Chinese Medicine, Guangzhou, Guangdong 510006, China

ARTICLE INFO

Article history:

Received 10 January 2015

Received in revised form 1 July 2015

Accepted 9 July 2015

Keywords:

Flickingeria fimbriata

Orchidaceae

Norditerpenoids

Absolute configuration

NF-κB

ABSTRACT

Chemical investigation of the aerial parts of *Flickingeria fimbriata* (Bl.) Hawkes resulted in isolation of sixteen *ent*-pimarane diterpenoids, including five rare 16-nor-*ent*-pimarane diterpenoids, two 15,16-dinor-*ent*-pimarane diterpenoids and one *ent*-pimarane diterpenoid. Structures were mainly elucidated by extensive spectroscopic analysis, and their absolute configurations were unequivocally determined by the exciton chirality method, the modified Mosher's method, the CD experiments (including Sznatzke's method) and chemical transformations, respectively. All the isolated compounds were screened for inhibitory effects on the nuclear factor-kappaB (NF-κB) in lipopolysaccharide (LPS) induced murine macrophage RAW264.7 cells, using a NF-κB-dependent luciferase reporter gene assay. Several of these compounds displayed comparable or even better activities than the positive control pyrrolidinedithiocarbamate (PDTC) (IC₅₀ = 26.3 μM) with IC₅₀ values in the range of 14.7–29.2 μM and structure–activity relationships are briefly proposed.

© 2015 Elsevier Ltd. All rights reserved.

1. Introduction

Flickingeria fimbriata (Bl.) Hawkes belongs to the medically important genus *Flickingeria* (Orchidaceae), which includes approximately seventy species. It is well known as an effective succedaneum for the precious and scarce congener *Dendrobium candidum* for treatment of inflammatory diseases, such as pneumonia, tuberculosis, bronchitis, asthma and pleurisy (Song, 1999). In a continuing search for bioactive metabolites from *F. fimbriata* (Chen et al., 2014a, 2014b), five new norditerpenoids (**1–5**) representing rare examples of 16-nor-*ent*-pimaranes, two new dinorditerpenoids (**6–7**) possessing a skeleton of 15,16-dinor-*ent*-pimarane, and one new *ent*-pimarane diterpenoid glycoside (**11**), along with eight known analogs (**8–10** and **12–16**) were isolated. Their structures, including absolute configurations, were determined on the basis of detailed spectroscopic analysis and various forms of chemical evidence. The absolute configuration of the known compound **10** was first elucidated by a CD experiment.

* Corresponding authors at: School of Pharmaceutical Sciences, Sun Yat-sen University, Guangzhou, Guangdong 510006, China.

E-mail addresses: lssydp@mail.sysu.edu.cn (D.-p. Yang), zhaozhm2@mail.sysu.edu.cn (Z.-m. Zhao).

Nuclear transcription factor kappa-B (NF-κB) is a transcription factor that is involved in activating large numbers of genes corresponding to challenges by infections, inflammation, and other stressful situations; this results in rapid reprogramming of gene expression (Rothwarf and Karin, 1999; DiDonato et al., 2012). As a key regulator, NF-κB regulate many pro-inflammatory pathways via the regulation of genes that encode pro-inflammatory cytokines, adhesion molecules, chemokines, growth factors and inducible enzymes (Lawrence et al., 2001; Tornatore et al., 2012); therefore, its inhibition results in anti-inflammatory effects.

Combined with the widely reported anti-inflammatory activities of *ent*-pimarane diterpenoids *in vitro* (Wu et al., 2014; Costantino et al., 2009) as well as in animal models (Possebon et al., 2014), compounds **1–16** were evaluated for their NF-κB signaling pathway suppression effects on LPS-induced murine macrophage RAW264.7 cells using the NF-κB-dependent luciferase reporter gene assay. Compounds **11**, **13** and **15–16** exhibited comparable inhibitory activities with IC₅₀ values between 26.9 and 29.2 μM; compounds **4** and **6–7** were more active than the positive control PDTC (IC₅₀ = 26.3 μM) with IC₅₀ values in the range 14.7–19.2 μM. Herein, details of the isolation, structural elucidation, and NF-κB inhibitory activity as well as preliminary structure–activity relationships of these compounds are described.

2. Results and discussion

2.1. Structure elucidation and identification

The methanol extract of the dried aerial parts of *F. fimbriata* was suspended in H₂O and successively partitioned with EtOAc and *n*-BuOH. Various column chromatographic separations (MCI, silica gel, Sephadex LH-20 and a reversed-phase ODS-A) of the EtOAc and *n*-BuOH extracts afforded sixteen *ent*-pimarane diterpenoids, including five new norditerpenoids (**1–5**), two new dinorditerpenoids (**6–7**) and one new diterpenoid glycoside (**11**) (Fig. 1).

Compound **1** was obtained as a colorless oil. Its molecular formula was established as C₁₉H₃₀O₄ based on a quasimolecular ion peak at *m/z* 345.2048 [M+Na]⁺ (calcd for C₁₉H₃₀O₄Na, 345.2036) in the positive HRESIMS measurement establishing five degrees of unsaturation. The IR absorption bands at 3381 and 1708 cm⁻¹ indicated the presence of hydroxyl and carbonyl groups, respectively. The ¹H NMR spectrum of **1** showed four tertiary methyls [δ_H 0.78, 0.83, 1.02 and 1.19, each (3H, s)], two oxygenated methines [δ_H 2.95 (1H, d, *J* = 9.6 Hz) and 3.56 (1H, ddd, *J* = 4.2, 9.6, 12.2 Hz)], one olefinic proton (δ_H 5.42, br s) and a series of aliphatic methylene multiplets. The ¹³C NMR spectrum, in combination with DEPT experiments, displayed 19 carbon resonances, including four quaternary methyls, five methylenes, four methines (including two oxygenated carbons), two olefinic carbon, one carboxyl carbon and three quaternary carbons, respectively. As two of the five degrees of unsaturation were accounted for by a double bond and a carboxyl group, the remaining three degrees of unsaturation required a tricyclic nature of **1**. The aforementioned spectrum showed high similarity to that for the co-occurring known analog norflickinimiod A (**8**) (Chen et al., 2014a) except for chemical shifts of A-ring carbon atoms when combined with detailed 2D NMR spectroscopic analyses (HSQC, ¹H–¹H COSY and HMBC) (Fig. 2), structure **1** was confirmed as depicted. Its relative configuration was established by the NOESY correlations (Fig. 2) and coupling constants. The NOESY spectrum showed correlated signals of H-2/H₃-19, H-2/H₃-20 and H-6 α /H₃-20, which indicated that these protons were cofacial and axial oriented, assigned here as an α orientation. Correspondingly, OH-2 and H₃-18 were assigned to be in a β orientation, suggesting a chair conformation for ring A. Based on

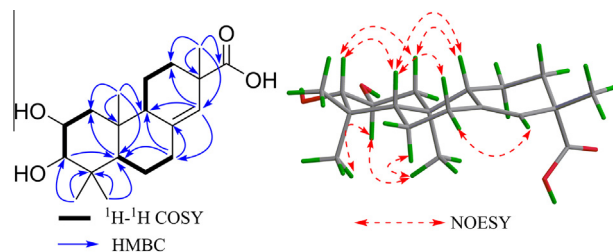


Fig. 2. Selected 2D NMR correlations of compound **1**.

the large coupling constant between H-2 and H-3 (*J*₃₋₂ = 9.6 Hz), the OH-3 group was assigned as being α . The β assignment of protons H-5 and H-9 were deduced from the NOE correlations of H-1 β /H-5, H-5/H-7 β and H-5/H-9. The absolute configuration at C-13 was assigned as *S* by analysis of the CD spectrum of **1** (Supplementary material, S63) matched well with that of **8**.

To determine the absolute configurations at C-2 and C-3, the exciton chirality method (Harada and Nakanishi, 1972) was applied. Benzoylation of **1** with benzoyl chloride afforded 2,3-*O*-dibenzoate (**1a**). The CD spectrum of **1a** (Fig. 3) in MeCN showed a pair of exciton split Cotton effects with a positive one centering at λ_{max} 237 nm ($\Delta\epsilon$ +12.0) and a negative one at λ_{max} 222 nm ($\Delta\epsilon$ -15.3), with a maximum absorption at λ_{max} 227 nm in its UV spectrum, which indicated that the transition dipole moments of the two benzoyl groups should be oriented clockwise in space and with a positive chirality (Fig. 3) on the basis of the dibenzoate chirality rule. These analyses allowed us to definitely establish 2*S* and 3*S* configurations. Considering the relative configuration established by the NOESY spectrum, compound **1** was determined as (2*S*,3*S*,5*S*,9*S*,10*S*,13*S*)-2,3-dihydroxy-16-nor-*ent*-pimar-8(14)-en-15-oic acid.

Compound **2**, a colorless oil, had a molecular formula C₁₉H₃₀O₃, as determined by the quasimolecular ion peak at *m/z* 329.2098 [M+Na]⁺ (calcd for C₁₉H₃₀O₃Na, 329.2087) in HRESIMS spectrum. Comparison of the NMR spectroscopic data of **2** (Tables 1 and 2) with those of **1** showed the differences, the main one being the presence of the oxygenated methine carbon (C-2, δ_C 69.4) in **1**

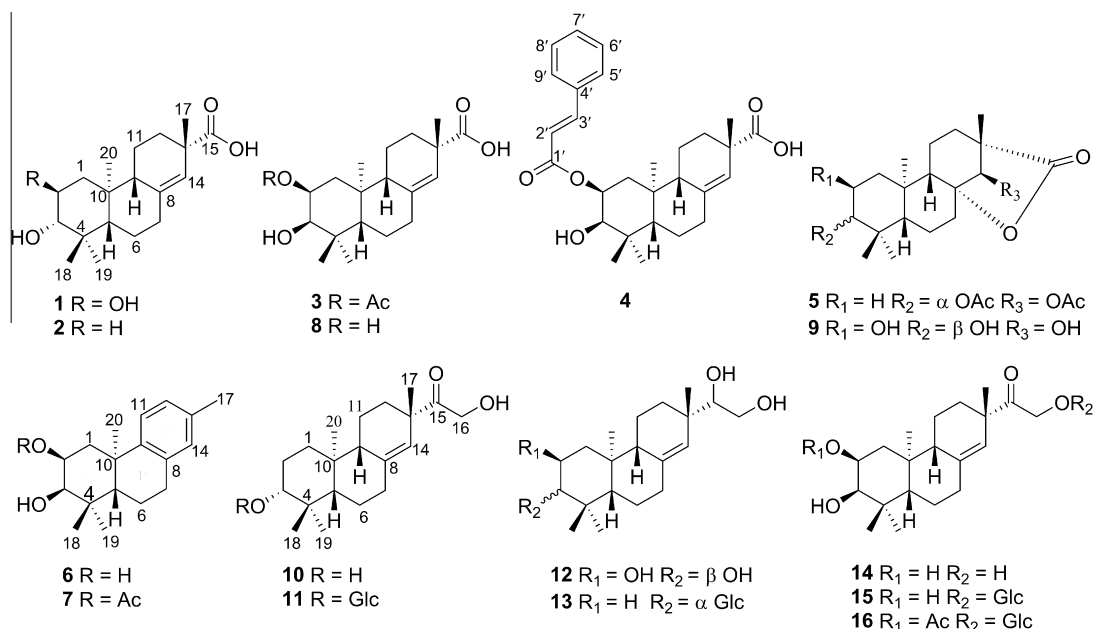


Fig. 1. Structures of isolated compounds **1–16**.

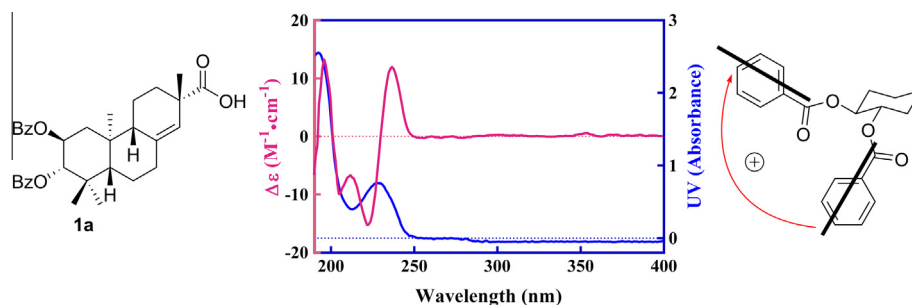


Fig. 3. CD and UV spectra of compound **1a** in MeCN. Red arrow denotes the electric transition dipole of the chromophores. (For interpretation of the references to colour in this figure legend, the reader is referred to the web version of this article.)

Table 1

¹H NMR spectroscopic data of compounds **1–7** and **11** (δ in ppm, mult, *J* in Hz).

Position	1 ^a	2 ^a	3 ^a	4 ^a	5 ^a	6 ^b	7 ^b	11 ^a
1 α	1.91 dd (4.2, 12.2)	1.69 m	1.78 t (12.2)	1.82 t (12.3)	1.72 m	2.28 m	2.26 m	1.70 m
1 β	1.13 d (3.2)	1.19 m	1.58 m	1.61 m	1.18 m	1.81 m	1.26 br s	1.18 m
2 α	3.56 ddd (4.2, 9.6, 12.2)	1.61 m	5.14, dd (1.8, 12.6)	5.24, ddd (2.5, 4.1, 12.6)	1.64 m	4.18 ddd (2.9, 4.4, 12.2)	5.39 ddd (2.5, 4.4, 12.4)	1.86 m
2 β	1.59 m	1.59 m	3.50 br s	3.54 d (1.8)	1.62 m	3.52 d (2.9)	3.59 d (2.5)	1.62 m
3	2.95 d (9.6)	3.20 dd (6.2, 10.2)			4.50 dd (6.2, 10.2)			3.42 dd (4.3, 12.5)
5	1.15 m	1.08 dd (2.2, 12.2)	1.56 m	1.57 m	1.02 m	1.73 m	1.84 dd (2.4, 12.5)	1.17 dd (2.6, 11.4)
6 α	1.42 dd (4.4, 12.7)	1.42 dd (4.2, 12.8)	1.55 overlap	1.57 m	1.64 m	1.79 m	1.81 m	1.75 m
6 β	1.63 m	1.64 m	1.45 m	1.40 m	1.61 m	1.74 m	1.76 m	1.51 m
7 α	2.33 ddd (1.8, 4.4, 13.5)	2.34 dd (2.4, 14.1)	2.38 d (13.7)	2.35 dd (3.3, 14.0)	1.86 m	2.90 m	2.89 m	2.12 m
7 β	2.06 td (5.4, 13.5)	2.05 td (5.1, 13.4)	2.12 m	2.10 m	1.68 m	2.85 m	2.85 m	2.42 m
9	1.79 t (8.6)	1.71 m	1.94 t (8.4)	1.94 t (8.5)	1.58 m			1.78 m
11 α	1.48 td (3.3, 13.8)	1.48 m	1.65 m	1.66 m	1.42 m	7.15 d (8.0)	7.10 d (8.0)	1.19 m
11 β	1.65 m	1.62 m	2.05 m	1.42 m	1.37 m			1.61 dd (3.3, 10.4)
12 α	1.13 d (3.2)	1.08 dd (2.2, 12.2)	1.18 d (13.4)	1.16 m	1.43 m	6.94 dd (1.3, 8.0)	6.93 dd (1.3, 8.0)	2.31 m
12 β	2.16 dt (3.5, 12.9)	2.16 d (11.2)	2.19 d (12.8)	2.16 m	1.80 m			1.12 m
14	5.42 br s	5.43 br s	5.46 br s	5.41 br s	4.85 br	6.87 (1.3)	6.87 (1.3)	5.51 br s
16a								4.40 s
16b								4.43 s
17	1.19 s	1.17 s	1.23 s	1.18 s	1.07 s	2.26 s	2.27 s	1.12 s
18	1.02 s	1.00 s	1.03 s	1.02 s	1.02 s	1.09 s	1.10 s	1.08 s
19	0.83 s	0.81 s	0.98 s	0.99 s	0.95 s	0.97 s	1.03 s	0.88 s
20	0.78 s	0.75 s	0.86 s	0.83 s	0.92 s	1.21 s	1.27 s	0.74 s
2-OOCH ₃			2.08 s				2.13 s	
3-OOCH ₃					2.03 s			
14-OOCCH ₃					2.18 s			
Glc 1'								4.35 d (7.7)
2'								3.18 dd (7.7, 9.1)
3'								3.39 dd (2.7, 4.0)
4'								3.30 d (8.6)
5'								3.27 dd (2.3, 5.6)
6'a								3.69 dd (5.7, 11.8)
6'b								3.88 dd (2.3, 11.8)

^a Measured in 400 MHz, in CH₃OH.

^b Measured in 400 MHz, in CHCl₃.

which was replaced the one sp³ methine carbon (C-2, δ_C 28.4) in **2**. The variation of the substituent at C-2 from compound **1** to **2** was supported by the crucial ¹H–¹H COSY correlations of H-1/H₂-2 and H₂-2/H-3. Detailed analysis of the NMR spectroscopic data of **2** also suggested high structural similarity to the already known compound **10**, lonchophylloid B (Ma et al., 1998), with the major

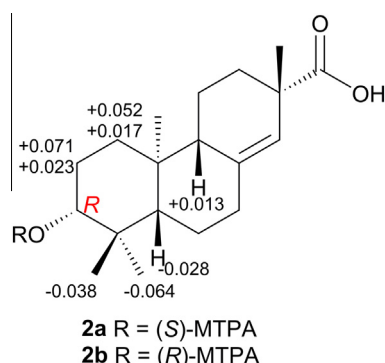
differences due to the presence of one carbonyl (C-15) and one oxygenated methylene (C-16) in **10** being replaced by one carboxyl (C-15) in **2**, as evidenced by the HMBC correlation from H₃-17 (δ_H 1.17) to C-15 (δ_C 181.3) in **2**. Structure **2** was thus deduced as depicted. H-3 was assigned a β -equatorial orientation, based on the coupling constants ($J_{3-2} = 6.2, 10.2$ Hz) and the NOESY

Table 2
¹³C NMR data of compounds **1–7** and **11** (δ in ppm, type).

Position	1 ^a	2 ^a	3 ^a	4 ^a	5 ^a	6 ^b	7 ^b	11 ^a
1	46.8, CH ₂	38.7, CH ₂	37.7, CH ₂	37.8, CH ₂	38.5, CH ₂	40.4, CH ₂	36.5, CH ₂	37.9, CH ₂
2	69.4, CH	28.4, CH ₂	72.3, CH	72.3, CH	24.5, CH ₂	67.2, CH	71.6, CH	24.4, CH ₂
3	84.3, CH	79.9, CH	77.4, CH	77.6, CH	82.2, CH	79.0, CH	76.8, CH	86.0, CH
4	40.8, C	40.2, C	40.1, C	40.2, C	38.9, C	38.5, C	38.7, C	39.5, C
5	55.5, CH	55.7, CH	48.9, CH	48.9, CH	54.9, CH	43.1, CH	43.1, CH	56.0, CH
6	23.5, CH ₂	23.5, CH ₂	22.9, CH ₂	23.0, CH ₂	19.4, CH ₂	18.6, CH ₂	18.5, CH ₂	23.4, CH ₂
7	36.7, CH ₂	36.9, CH ₂	36.7, CH ₂	36.7, CH ₂	35.1, CH ₂	30.2, CH ₂	30.1, CH ₂	36.9, CH ₂
8	139.6, C	139.1, C	139.8, C	136.0, C	85.1, C	134.8, C	134.9, C	143.1, C
9	52.1, CH	52.3, CH	51.8, CH	51.8, CH	47.3, CH	146.4, C	146.2, C	52.2, CH
10	40.2, C	39.5, C	40.4, C	40.6, C	37.6, C	38.7, C	38.8, C	39.4, C
11	21.7, CH ₂	21.7, CH ₂	21.5, CH ₂	21.5, CH ₂	19.5, CH ₂	124.2, CH	124.1, CH	21.4, CH ₂
12	34.4, CH ₂	34.9, CH ₂	34.4, CH ₂	34.5, CH ₂	28.6, CH ₂	126.8, CH	126.8, CH	33.9, CH ₂
13	44.2, C	44.8, C	44.1, C	44.4, C	47.0, C	135.1, C	135.2, C	48.3, C
14	127.8, CH	128.4, CH	127.8, CH	127.4, CH	78.7, CH	129.8, CH	129.9, CH	125.3, CH
15	181.1, C	181.3, C	180.9, C	179.3, C	178.7, C			215.7, C
16								66.8, CH ₂
17	28.3, CH ₃	28.7, CH ₃	28.3, CH ₃	28.1, CH ₃	19.0, CH ₃	21.0, CH ₃	21.0, CH ₃	27.9, CH ₃
18	29.7, CH ₃	29.2, CH ₃	29.4, CH ₃	29.4, CH ₃	29.0, CH ₃	28.5, CH ₃	28.4, CH ₃	29.2, CH ₃
19	17.7, CH ₃	16.6, CH ₃	22.8, CH ₃	22.8, CH ₃	17.6, CH ₃	21.8, CH ₃	21.9, CH ₃	17.4, CH ₃
20	15.9, CH ₃	15.3, CH ₃	15.9, CH ₃	15.8, CH ₃	15.6, CH ₃	25.8, CH ₃	25.7, CH ₃	15.1, CH ₃
2-OCCH ₃			21.4, CH ₃				21.6, CH ₃	
2-OCCCH ₃			172.7, C				170.5, C	
3-OCCH ₃					21.2, CH ₃			
3-OCCCH ₃					172.9, C			
14-OCCH ₃					20.9, CH ₃			
14-OCCCH ₃					171.6, C			
Glc 1'								102.1, CH
2'								75.3, CH
3'								78.4, CH
4'								72.0, CH
5'								77.8, CH
6'								63.2, CH ₂

^a Measured in 100 MHz, in CH₃OH.^b Measured in 100 MHz, in CHCl₃.

correlation of H-3/H-5. The relative configurations of other chiral centers were the same as those of **1** based on the NOESY spectrum (Supplementary material, S13). The absolute configuration at C-13 (13S) was the same as compound **1**, this being confirmed by the well matched CD curves (Supplementary material, S63). The absolute configuration of the chiral centre at C-2 was confirmed by the modified Mosher's method (Ohtani et al., 1991; Wang et al., 2013a,b). Esterification of **2** with *R*-(-)- and *S*-(+)-MTPA chlorides directly in an NMR tube led to *S*-MTPA ester (**2a**) and *R*-MTPA ester (**2b**), respectively. As shown in Fig. 4, the $\Delta\delta_H$ ($\Delta\delta_H = \delta_S - \delta_R$) values obtained from the proton signals assigned for these esters clearly indicated that the absolute configuration at C-3 was *R*. Combined with the relative configuration, compound **2** was established as (3*R*,5*S*,9*S*,10*S*,13*S*)-2-hydroxy-16-nor-*ent*-pimar-8(14)-en-15-oic acid.

**Fig. 4.** The $\Delta\delta_H$ values ($\Delta\delta_H = \Delta\delta_S - \Delta\delta_R$) for *S*-/*R*-MTPA esters of compound **2**.

Compound **3**, a colorless gum, had a molecular formula C₂₁H₃₂O₅ as determined by the *m/z* of 387.2146 [M+Na]⁺ (calcd 387.2142) from HRESIMS. Its NMR spectroscopic data (Tables 1 and 2) showed high similarity to those of compound **8** except for the presence of an additional acetyl [δ_H 2.08 (s, 3H), δ_C 21.4 and 172.7] in **3**, suggesting it was an acetylated derivative of **8**. The acetoxy group was assigned at C-2 by the key HMBC correlation from H-2 (δ_H 5.14) to the acetyl carbonyl at δ_C 172.7, which was further supported by up-field shifts of C-1 and C-3 signals and severely down field-shifted proton signal of H-2 (δ_H 5.14) in **3** with respect to those in **8**. The absolute configuration of **3** was determined to be the same as that of **8** by a successful chemical conversion of **3** to **8** via alkaline hydrolysis. Therefore, structure **3** was characterized as (2*S*,3*R*,5*S*,9*S*,10*S*,13*S*)-2-acetoxy-3-hydroxy-16-nor-*ent*-pimar-8(14)-en-15-oic acid.

Compound **4** was obtained as a colorless amorphous gum. Its molecular formula was established as C₂₈H₃₆O₅ based on the positive-ion HRESIMS with a *m/z* of 475.2468 [M+Na]⁺. Its ESI mass spectrum exhibited a peak (*m/z* 131, [C₈H₇CO]⁺) attributed to a cinnamoyl group (Bai et al., 2012), this being assigned as a *E*-cinnamoyl group by analysis of the ¹H and ¹³C NMR data, which included signals for five aromatic protons [δ_H 7.60 (2H, H-5' and H-9') and 7.40–7.42 (3H, H-6', H-7' and H-8')], two olefinic protons [δ_H 6.56 (1H, d, *J* = 16.0 Hz, H-2') and 7.74 (1H, d, *J* = 16.0 Hz, H-3')], six aromatic carbons [δ_C 136.0 (C-4'), 129.4 (C-5' and C-9'), 130.2 (C-6' and C-8') and 131.6 (C-7')], two olefinic carbons [δ_C 119.5 (C-2') and 146.3 (C-3')] and a carbonyl carbon at δ_C 168.4 (C-1') (Allouche et al., 2009; Wang et al., 2013a,b). The NMR spectroscopic data of **4** closely resembled those of **8**, except for the presence of an additional cinnamoyl group. The cinnamoyl group was located at C-2 supported by the HMBC correlation from H-2

(δ_H 5.24) to the carbonyl carbon C-1' (δ_C 168.4). The relative configuration of **4** was the same as that of **8** according to NOESY correlations (Supplementary material, S62). Likewise, the absolute configuration at C-13 was assigned as *S* based on the negative Cotton effect at 228 ($\Delta\epsilon$ -1.44) nm in its CD spectrum (Fig. 5) being consistent with those of compounds **1–3**.

The absolute stereochemistry of **4** was also elucidated using the CD exciton chirality method (Harada et al., 1981). Its UV spectrum (Fig. 5) showed a strong absorption at λ_{\max} 274 ($\log\epsilon$ 4.39) attributable to the *trans*-cinnamoyl group. Corresponding to this UV maximum, the CD spectrum of **4** (Fig. 5) exhibited a negative Cotton effect at λ_{\max} 280 nm ($\Delta\epsilon$ -19.14), this arising from the vinyl benzene moiety, and a split Cotton effect between the two different chromophores of the conjugated α,β -unsaturated ketone (260 nm, $\Delta\epsilon$ +6.96, π - π^* transition) and the $\Delta^{8,14}$ double bond (206 nm, $\Delta\epsilon$ -9.41, π - π^* transition) (Zhang et al., 2011; Liu et al., 2012). This indicated that the transition dipole moments of the two different chromophores were oriented clockwise in space and with a positive chirality (Fig. 5). Thus, the absolute configurations of the related chiral centers were concluded as being 2*S*, 3*R*, 5*S*, 9*S* and 10*S*. Ultimately, the stereostructure of **4** was further supported by alkaline hydrolysis from **4** to afford **8**. Compound **4** was named as (2*S*,3*R*,5*S*,9*S*,10*S*,13*S*)-2-*O-E*-cinnamoyl-3-hydroxy-16-nor-*ent*-pimar-8(14)-*en*-15-oic acid.

The HRESIMS analysis of compound **5** showed a molecular formula of $C_{23}H_{34}O_6$ as established by the m/z of 429.2264 [$M+Na$]⁺ (calcd for $C_{23}H_{34}O_6Na$, 429.2248) with seven unsaturations. Careful comparison of the 1H and ^{13}C NMR spectroscopic data of **5** (Tables 1 and 2) with those of co-occurring compound **9**, norflickinlimiod B (Chen et al., 2014a), established that the main differences were due to the oxygenated carbon at C-2 in **9** replaced by one sp^3 methine carbon (δ_C 24.5, C-2) and to the presence of two additional acetyl groups [δ_H 2.03 (s, 3H), δ_C 21.2 and 172.9; δ_H 2.18 (s, 3H), δ_C 20.9 and 171.6] in **5**. The two acetoxy groups were connected to C-3 and C-14, respectively, as established by the core HMBC correlations from H-3 (δ_H 4.50) to the acetyl carbonyl at δ_C 172.9 and from H-14 (δ_H 4.85) to the acetyl carbonyl at δ_C 171.6. The determination of β -equatorial orientation of H-3 was also concluded from the coupling constants (J_{3-2} = 6.2, 10.2 Hz) and the NOESY correlations of H-3/H-5 and H-3/H-1 β . The relative configuration of 14-OOCCH₃ was assigned as β , this being deduced from the NOE correlations of 14-OOCCH₃/H-9 and 14-OOCCH₃/H-7 β . Other chiral centers were the same as for compound **9**, as confirmed by the NOESY correlations (Supplementary material, S62). The CD curve of **5** (Supplementary material, S63) was very similar to that of **9**, indicative of a 13*S* configuration. Thus, structure **5** was determined as 3 α ,14 β -diacetoxy-16-nor-*ent*-pimar-15 α ,8-olide, i.e. the corresponding diacetate derivative of norflickinlimiod C (Chen et al., 2014a) previously reported from this plant.

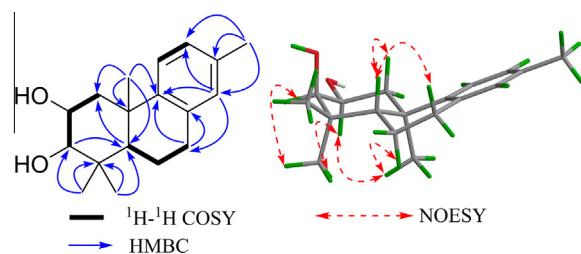


Fig. 6. Selected 2D NMR correlations of compound **6**.

Compound **6** was isolated as a colorless oil, whose molecular formula was established as $C_{18}H_{26}O_2$ based on a quasimolecular ion peak at m/z 297.1836 [$M+Na$]⁺ (calcd for $C_{18}H_{26}O_2Na$, 297.1825) in the positive HRESIMS measurements. Analysis of its NMR spectroscopic data (Tables 1 and 2) indicated high structural similarity with the known flickinlimilin B (Chen et al., 2014b), except that the keto function at C-7 position of flickinlimilin B was replaced by a sp^3 methine carbon in **6**. This variation was confirmed by the pivotal HMBC correlation from H-14 [δ_H 6.87 (1H, d, J = 1.3 Hz)] to C-7 (δ_C 30.2) in **6**. The relative configuration can also be established by analyzing the NOESY correlations (Fig. 6) and coupling constants. The NOESY spectrum showed correlated signals of H-2/H₃-19, H-2/H₃-20, H-6 α /H₃-20, and therefore H-2 group was assigned as α . Correspondingly, OH-2 and H₃-18 were β -oriented. The OH-3 group was assigned as being β -oriented on the basis of the small coupling constants between H-2 and H-3 (J = 2.9 Hz). The β assignment of H-5 was deduced from the NOE correlation of H-1 β and H-5.

Since the diester derivative necessary for CD exciton chirality method was difficult to synthesize probably due to the steric hindrance and since the Cotton effect was not observed in the CD spectrum of **6**, the exciton chirality method and ECD calculation were not suitable for determination of the absolute configurations of compound **6** at C-2 and C-3. Therefore, an *in situ* dimolybdenum CD method developed by Snatzke and Frelek (Snatzke et al., 1981; Frelek et al., 1999; Di Bari et al., 2001; Liu et al., 2014) was employed. According to the empirical helicity rule proposed by Snatzke, the conformation of a chiral metal complex required the vicinal diol to be in a *gauche* arrangement and which would give two diastereomorphous structures, where the favored conformation prefers the bulkier groups in a *pseudo*-equatorial position away from the remaining portion of the metal complex. Consequently, the positive Cotton effect at λ_{\max} 302 nm ($\Delta\epsilon$ +0.354) in the induced CD spectrum of the metal complex of compound **6** in anhydrous DMSO (Fig. 7) unambiguously permitted assignment of 2*S* and 3*R* configurations. Taking the relative configuration into account, the absolute configurations was assigned as

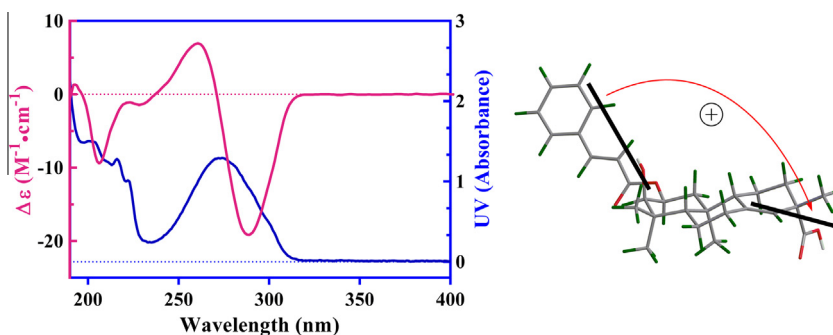


Fig. 5. CD and UV spectra of compound **4** in MeCN. Red arrow denotes the electric transition dipole of the chromophores. (For interpretation of the references to colour in this figure legend, the reader is referred to the web version of this article.)

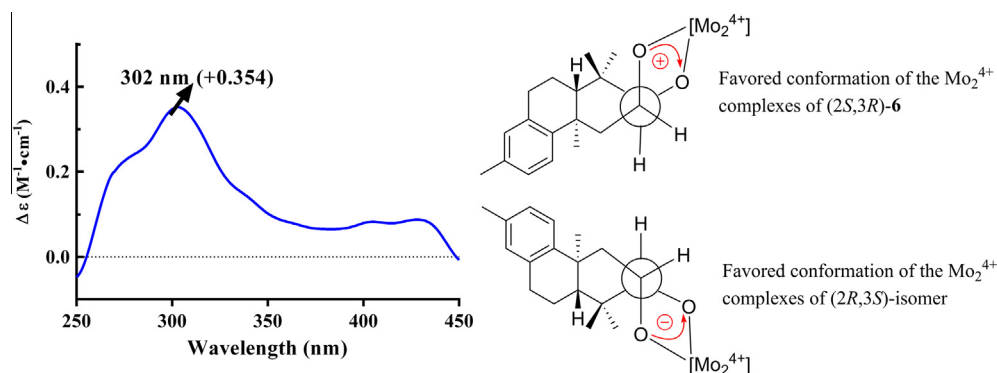


Fig. 7. The $\text{Mo}_2(\text{OAc})_4$ induced CD spectrum of compound **6** in anhydrous DMSO and favored conformations of the Mo_2^{4+} complexes of compound **6** and its isomer.

2*S*, 3*R*, 5*S* and 10*R* and compound **6** was named as (2*S*,3*R*,5*S*,10*R*)-2,3-dihydroxy-15,16-dinor-*ent*-pimar-8,11,13-triene.

Compound **7** was isolated as a colourless oil and its molecular formula was determined to be $\text{C}_{20}\text{H}_{28}\text{O}_3$ by HRESIMS measurements for the m/z 339.1935 ($\text{C}_{20}\text{H}_{28}\text{O}_3\text{Na}$, calcd 339.1931) with 42 mass units higher than that of **6**. Its ^1H and ^{13}C NMR spectroscopic data (Tables 1 and 2) closely resembled those of **6** except for the presence of signals for an acetyl group [δ_{H} 2.13 (3H, s), δ_{C} 21.6 and 170.5], indicating that **7** was acetylated derivative of **6**. The acetoxy group was assigned at C-2 by the HMBC correlation from H-2 (δ_{H} 5.39) to the acetyl carbonyl at δ_{C} 170.5, which was further supported by the up-field shifts C-1 and C-3 signals and the obvious down field-shifted proton signal of H-3 (δ_{H} 5.44) in **7** with respect to those in **6**. The stereochemical structure of **7** was also confirmed by alkaline hydrolysis of **7**, which yielded the hydrolysis product confirmed as compound **6** by ^1H NMR, R_f values and specific rotation. Then the structure of compound **7** was (2*S*,3*R*,5*S*,10*R*)-2-acetoxy-3-hydroxy-15,16-dinor-*ent*-pimar-8,11,13-triene.

Known compound **10** was identified as lonchophylloid B by comparison of its ^1H , ^{13}C NMR and optical rotation data with those of the literature (Ma et al., 1998), while the relative configuration of this compound has been determined by the NOE difference spectrum and X-ray diffraction method, the determination of the absolute configuration was achieved here by means of the CD experiment. The observed CD curve of compound **10** (Supplementary material, S64) exhibited highly similar Cotton effects with those of 2-acetyl-flickinflimiod (Chen et al., 2014a), indicating that the absolute configuration at C-13 was *S*. Based on this result, the absolute configuration can be determined as 3*R*, 5*S*, 9*S*, 10*S* and 13*S*.

Compound **11** was obtained as an optically active colorless gum with a molecular formula of $\text{C}_{26}\text{H}_{42}\text{O}_8$ as determined by the m/z of 505.2760 [$\text{M}+\text{Na}$] $^+$ (calcd 505.2772) from HRESIMS. Its ^1H and ^{13}C NMR data (Tables 1 and 2) resembled those of **10**, except for the presence of additional signals being attributed to a typical β -glucopyranose moiety [δ_{H} 4.35 (1H, d, $J=7.7$ Hz, H-1'), 3.69 (1H, dd, $J=5.7, 11.8$ Hz, H-6'a) and 3.88 (1H, dd, $J=2.3, 11.8$ Hz, H-6'b); δ_{C} 102.1 (CH, C-1') and 63.8 (CH_2 , C-6')], indicating **11** was a glycosylated derivative of **10**. The glucopyranose moiety was connected to C-3 as evidenced by the mutual HMBC correlations from H-3 (δ_{H} 3.42, dd, $J=4.3, 12.2$ Hz) to C-1' (δ_{C} 102.1), and from H-1' (δ_{H} 4.35, d, $J=7.7$ Hz) to C-3 (δ_{C} 86.0). Furthermore, this was supported by the down field-shifted carbon signal of C-3 (δ_{C} 86.0) in **11**, as compared to **10** (δ_{C} 79.2). Acid hydrolysis of **11** with 2 M HCl gave a diterpene and glucose. The diterpene was confirmed to be **10** by 1D NMR spectroscopic data and optical rotation. The absolute configuration of the β -glucose was identified to be of the D-configuration by HPLC analysis after

conversion of the sugar to the thiocarbamoyl-thiazolidine derivative (Tanaka et al., 2007; Wang et al., 2013a,b). The CD spectrum of **11** (Supplementary material, S64) displayed remarkably similar Cotton effects with those of **10**. Therefore, compound **11** was identified and named as (3*R*,5*S*,9*S*,10*S*,13*S*)-3,16-dihydroxyl-15-one-*ent*-pimar-8(14)-ene-3-O- β -D-glucopyranoside.

The structures of known compounds were elucidated by spectrometric methods (^1H NMR, ^{13}C NMR, 2D NMR and ESIMS) and by comparison with literature data as norflickinflimiod A (**8**), norflickinflimiod B (**9**), flickinflimioside A (**16**) and flickinflimioside B (**15**) previously reported from the dried stems of *F. fimbriata* (Chen et al., 2014a), lonchophylloid B (**10**) (Ma et al., 1998) from fresh stems of *Ephemerantha lonchophylla*, darutoside (**13**) from aerial parts of *Siegesbeckia pubescens* (Wang et al., 2010), 2 β ,3 β ,15,16-tetrahydroxy-*ent*-pimar-8(14)-en (**12**) and 2 β ,3 β ,16-trihydroxy-*ent*-pimar-8(14)-en-15-one (**14**) previously isolated from aerial parts of *Milleria quinqueflora* (Jakupovic et al., 1987), respectively (Fig. 1).

2.2. Biological evaluation

Compounds **1–16** were tested for their abilities to inhibit the NF- κ B pathway in LPS stimulated RAW264.7 cells using the NF- κ B-dependent luciferase reporter gene assay (Moon et al., 2001; Xu et al., 2013). Compounds **3**, **5** and **8–9** were inactive (<50% inhibition at 50 μM), while compounds **4** and **6–7** exhibited pronounced inhibition with IC_{50} values in the range of 14.7–19.2 μM , i.e. being more active than the positive control PDTC ($\text{IC}_{50} = 26.3$ μM), a well-known NF- κ B inhibitor (Table 3). Compounds **11**, **13** and **15–16** showed potential inhibitory activities with IC_{50} values of 26.9–29.2 μM , and compounds **1**, **2**, **10**, **12** and **14** displayed moderate suppression with IC_{50} values ranging from 30.4–43.7 μM .

Preliminary structure–activity relationships could be concluded from the inhibition results. For the 16-nor-*ent*-pimarane diterpenoids, the orientation of 3-OH (α and β) had a slight impact on

Table 3
 IC_{50} values of the active compounds against NF- κ B.

Compound	IC_{50} (μM)	Compound	IC_{50} (μM)
1	38.3 \pm 2.2	12	38.8 \pm 2.3
2	43.7 \pm 1.2	13	28.4 \pm 2.7
4	14.7 \pm 1.8	14	33.8 \pm 2.9
6	18.3 \pm 1.3	15	29.2 \pm 2.1
7	19.2 \pm 0.9	16	27.5 \pm 1.6
10	30.4 \pm 1.7	PDTC ^a	26.3 \pm 1.2
11	26.9 \pm 1.7		

^a Positive control.

inhibition (**3** and **7**, no activity; **1–2**, moderate inhibition), and cinnamoylation of the –OH group at C-2 resulted in a significant increase of the inhibitory effect (**4**, $IC_{50} = 14.9 \mu\text{M}$); for the C-ring aromatized-15,16-dinor-*ent*-pimarane diterpenoids, acetylation of the –OH group at C-2 resulted in a tiny decrease of inhibition (**7**, $IC_{50} = 19.2 \mu\text{M}$); for the *ent*-pimarane diterpenoids, glycosides (**11**, **13** and **15–16**) displayed much better inhibitory activities than the corresponding aglycones (**10**, **12** and **14**), indicated that β -glucose moiety is clearly necessary for inhibitory activity.

3. Conclusions

In this study, sixteen diterpenoids including five new rare 16-nor-*ent*-pimarane diterpenoids (**1–5**), two new 15,16-dinor-*ent*-pimarane diterpenoids (**6–7**) and one new *ent*-pimarane diterpenoid glycoside (**11**) were isolated and identified from the aerial parts of *F. fimbriata*. In the luciferase assay, compounds **4** and **6–7** exhibited pronounced NF- κ B inhibitory activities with IC_{50} values in the range of 14.7–19.2 μM , being more active than the positive control PDTC ($IC_{50} = 26.3 \mu\text{M}$). Up to now, only about ten naturally occurring 16-nor-*ent*-pimarane diterpenoids have been reported, thus this work extends the chemical and biological diversity of this type of norditerpenoids. As the NF- κ B-suppression activity results in anti-inflammatory effects, the evaluation of these active compounds may provide some scientific basis for the anti-inflammatory efficacy of this medicinal plant.

In addition, to the best of our knowledge, *ent*-pimarane norditerpenoids from the *Flickingeria* genus have only been reported in *F. fimbriata*, suggesting these norditerpenoids could be considered as chemotaxonomic markers.

4. Experimental

4.1. General

Optical rotations were measured on a Rudolph Autopol I automatic polarimeter, whereas UV spectra were obtained on a Shimadzu UV-2450 spectrophotometer. CD spectra were recorded on an Applied Photophysics Chirascan spectrometer. IR spectra were determined on a Perkin Elmer FT-IR Spectrum Two spectrometer. NMR spectra were measured on a Bruker AM-400 spectrometer at 25 °C. ESIMS was measured on a Finnigan LC QDECA instrument, and HRESIMS was performed on a Waters-Micromass Q-TOF. A Shimadzu LC-20 AT equipped with a SPD-M20A PDA detector was used for HPLC. Silica gel (300–400 mesh, Qingdao Haiyang Chemical Co., Ltd., Qingdao, China), C18 reversed-phase silica gel (12 nm, S-50 mm, YMC Co., Ltd, Japan), Sephadex LH-20 gel (Amersham Biosciences) and MCI gel (CHP20P, 75–150 mm, Mitsubishi Chemical Industries Ltd., Kyoto, Japan) were used for column chromatography (CC). All solvents used were of analytical grade (Guangzhou Chemical Reagents Company, Ltd., Guangzhou, China). For the NF- κ B biological assay: RAW264.7 cells (The Center of Cellular Resource, Chinese Academy of Science, Shanghai, China), Dulbecco's modified Eagle medium (DMEM) (Invitrogen-Gibco, Grand Island, NY), FBS (Invitrogen-Gibco, Grand Island, NY), Luciferase assay system reagent (Promega, Madison, CA, USA), Automated microplate reader (Molecular Devices, Sunnyvale, CA, USA).

4.2. Plant materials

Aerial parts of *F. fimbriata* were collected from Foshan, Guangdong Province of China, in August 2013. The plant material was authenticated by Professor De-po Yang and a plant specimen

has been deposited in the School of Pharmaceutical Sciences, Sun Yat-sen University (voucher specimen number: GDLSJ201308).

4.3. Extraction and isolation

Air-dried powder of aerial parts of *F. fimbriata* (4.5 kg) was extracted with MeOH (3 \times 15 L) by maceration at room temperature to afford a crude extract (350 g), which was suspended in H₂O (2.5 L) and successively partitioned with EtOAc (3 \times 2.5 L) and *n*-BuOH (3 \times 2.5 L). The EtOAc layer (83 g) was applied to MCI column ($L = 500 \text{ mm } \phi = 100 \text{ mm}$) eluting with MeOH/H₂O (10:90–100:0) to afford five fractions (Fr. E1–E5) on the basis of TLC analyses. Fr. E4 (12 g) was subjected to silica gel CC and eluted with CH₂Cl₂/MeOH successively to afford five fractions (Fr. E4a–E4e). Fr. E4c was separated by silica gel CC and Sephadex LH-20 CC (CHCl₃/MeOH, 1:1) to afford compound **7** (14 mg) and another fraction, which was successively subjected to reversed-phase ODS-A CC (MeOH/H₂O, 60:40–100:0) and repeated silica gel CC eluted with petroleum ether/EtOAc (6:1–1:2) to attain compounds **6** (8 mg) and **5** (8 mg). Fr. E4e was purified by Sephadex LH-20 CC (CHCl₃/MeOH, 1:1) followed by reversed-phase ODS-A CC (MeOH/H₂O, 60:40–100:0) to afford compounds **10** (19 mg), **3** (37 mg) and **4** (7 mg). Fr. E3 (14 g) was separated on a reversed-phase ODS-A column (MeOH/H₂O, 50:50–100:0), followed by a Sephadex LH-20 CC (MeOH) to afford compound **2** (12 mg). Fr. E2 was applied to silica gel CC and eluted with CH₂Cl₂/MeOH (100:1–10:1) to give five fractions (Fr. E2a–E2e). Fr. E2a was subjected to silica gel CC eluted with petroleum ether/EtOAc (4:1–1:2) followed by reversed-phase ODS-A CC (MeOH/H₂O, 50:50–100:0) to afford compounds **8** (20 mg) and **9** (23 mg). Fr. E2b was further purified by silica gel CC (CH₂Cl₂/MeOH, 100:1–10:1) to give compounds **14** (60 mg) and **1** (8 mg). Fr. E2c was successively applied to a Sephadex LH-20 column (CHCl₃/MeOH, 1:1), a silica gel column eluted with petroleum ether/EtOAc (4:1–1:2) and a reversed-phase ODS-A column (MeOH/H₂O, 50:50–100:0) to obtain compound **12** (8 mg). The *n*-BuOH layer (170 g) was subjected to MCI CC eluting with MeOH/H₂O (0:100–100:0) to afford five fractions (Fr. B1–B5). Fr. B5 (17 g) was separated by repeated reversed-phase ODS-A CC (MeOH/H₂O, 10:90–50:50), Sephadex LH-20 column (MeOH) and silica gel CC eluted with CH₂Cl₂/MeOH (30:1–10:1) to obtain compounds **11** (30 mg), **13** (28 mg), **16** (37 mg) and **15** (40 mg), respectively.

4.3.1. (2S,3S,5S,9S,10S,13S)-2,3-dihydroxy-16-nor-*ent*-pimar-8(14)-*en*-15-oic acid (**1**)

Colorless oil; $[\alpha]_D^{25} -21.0$ (c 0.13, MeOH); UV (MeOH) λ_{max} ($\log \epsilon$) 205 (2.83) nm; CD (MeCN) (1.4×10^{-4} M) λ_{max} ($\Delta \epsilon$) 223 (–0.36) nm; IR (microscope) ν_{max} 3381, 2925, 2859, 1708, 1549, 1462, 1389, 1259, 1129, 1064, 951 and 757 cm^{-1} ; for ¹H and ¹³C NMR spectroscopic data, see Tables 1 and 2; HRESIMS m/z 345.2048 [M+Na]⁺ (calcd for C₁₉H₃₀O₄Na, 345.2036).

4.3.2. (3R,5S,9S,10S,13S)-2-hydroxy-16-nor-*ent*-pimar-8(14)-*en*-15-oic acid (**2**)

Colorless oil; $[\alpha]_D^{25} -14.6$ (c 0.1, MeOH); UV (MeOH) λ_{max} ($\log \epsilon$) 204 (2.81) nm; CD (MeCN) (1.6×10^{-4} M) λ_{max} ($\Delta \epsilon$) 214 (–0.45) nm; IR (microscope) ν_{max} 3393, 2931, 2849, 2847, 1699, 1457, 1388, 1243, 1031, 932, 793 and 750 cm^{-1} ; for ¹H and ¹³C NMR spectroscopic data, see Tables 1 and 2; HRESIMS m/z 329.2098 [M+Na]⁺ (calcd for C₁₉H₃₀O₃Na, 329.2087).

4.3.3. (2S,3R,5S,9S,10S,13S)-2-acetoxy-3-hydroxy-16-nor-*ent*-pimar-8(14)-*en*-15-oic acid (**3**)

Colorless gum; $[\alpha]_D^{25} -54.1$ (c 0.32, MeOH); UV (MeOH) λ_{max} ($\log \epsilon$) 204 (2.89) nm; CD (MeCN) (1.2×10^{-4} M) λ_{max} ($\Delta \epsilon$) 222

(−0.94) nm; IR (microscope) ν_{\max} 3381, 2931, 1701, 1454, 1367, 1243, 1026, 926 and 676 cm^{-1} ; for ^1H and ^{13}C NMR spectroscopic data, see Tables 1 and 2; HRESIMS m/z 387.2146 $[\text{M}+\text{Na}]^+$ (calcd for $\text{C}_{21}\text{H}_{32}\text{O}_5\text{Na}$, 387.2142).

4.3.4. (2S,3R,5S,9S,10S,13S)-2-O-E-cinnamoyl-3-hydroxy-16-nor-ent-pimar-8(14)-en-15-oic acid (**4**)

Colorless gum; $[\alpha]_{\text{D}}^{25}$ −50.3 (c 0.16, MeOH); UV (MeOH) λ_{\max} ($\log \epsilon$) 275 (4.23), 217 (4.13), 206 (4.11) nm; CD (MeCN) (5.3×10^{-5} M) λ_{\max} ($\Delta \epsilon$) 288 (−19.14), 260 (+6.96), 228 (−1.44), 206 (−9.41) nm; IR (microscope) ν_{\max} 3415, 2943, 2872, 1711, 1636, 1450, 1310, 1280, 1201, 1165, 1027, 766, 710 and 684 cm^{-1} ; for ^1H and ^{13}C NMR spectroscopic data, see Tables 1 and 2, the E-cinnamoyl group δ_{H} : 6.56 (1H, d, $J = 16.0$ Hz, H-2'), 7.74 (1H, d, $J = 16.0$ Hz, H-3'), 7.60 (2H, H-5' and H-9'), 7.40–7.42 (3H, H-6', H-7' and H-8'); δ_{C} : 168.4 (C-1'), 119.5 (C-2'), 146.3 (C-3'), 136.0 (C-4'), 129.4 (C-5' and C-9'), 130.2 (C-6' and C-8'), 131.6 (C-7'); HRESIMS m/z 475.2468 $[\text{M}+\text{Na}]^+$ (calcd for $\text{C}_{28}\text{H}_{36}\text{O}_5\text{Na}$, 475.2460).

4.3.5. 3 α ,14 β -diacetoxy-16-nor-ent-pimar-15 α ,8-olide (**5**)

Colorless oil; $[\alpha]_{\text{D}}^{25}$ −8.5 (c 0.16, MeOH); UV (MeOH) λ_{\max} ($\log \epsilon$) 206 (3.21) nm; CD (MeCN) (9.6×10^{-5} M) λ_{\max} ($\Delta \epsilon$) 224 (−0.13) nm; IR (microscope) ν_{\max} 2922, 2850, 1779, 1732, 1646, 1368, 1254, 1224, 1214, 1141, 1062, 975, 953 and 755 cm^{-1} ; for ^1H and ^{13}C NMR spectroscopic data, see Tables 1 and 2; HRESIMS m/z 429.2264 $[\text{M}+\text{Na}]^+$ (calcd for $\text{C}_{23}\text{H}_{34}\text{O}_6\text{Na}$, 429.2248).

4.3.6. (2S,3R,5S,10R)-2,3-dihydroxy-15,16-dinor-ent-pimar-8,11,13-triene (**6**)

Colorless oil; $[\alpha]_{\text{D}}^{25}$ +14.6 (c 0.16, MeOH); UV (MeOH) λ_{\max} ($\log \epsilon$) 216 (3.74), 207 (3.85) nm; $\text{Mo}_2(\text{OAc})_4$ -induced CD (DMSO) λ_{\max} ($\Delta \epsilon$) 302 (+0.354) nm; IR (microscope) ν_{\max} 3384, 2944, 1618, 1499, 1457, 1377, 1280, 1131, 1043, 992, 940, 890, 810 and 678 cm^{-1} ; for ^1H and ^{13}C NMR spectroscopic data, see Tables 1 and 2; HRESIMS m/z 297.1836 $[\text{M}+\text{Na}]^+$ (calcd for $\text{C}_{18}\text{H}_{26}\text{O}_2\text{Na}$, 297.1825).

4.3.7. (2S,3R,5S,10R)-2-acetoxy-3-hydroxy-15,16-dinor-ent-pimar-8,11,13-triene (**7**)

Colorless oil; $[\alpha]_{\text{D}}^{25}$ +25.5 (c 0.17, MeOH); UV (MeOH) λ_{\max} ($\log \epsilon$) 215 (3.73), 205 (3.84) nm; IR (microscope) ν_{\max} 3392, 2947, 1716, 1499, 1365, 1245, 1059, 1029, 860 and 814 cm^{-1} ; for ^1H and ^{13}C NMR spectroscopic data, see Tables 1 and 2; HRESIMS m/z 339.1935 $[\text{M}+\text{Na}]^+$ (calcd for $\text{C}_{20}\text{H}_{28}\text{O}_3\text{Na}$, 339.1931).

4.3.8. (3R,5S,9S,10S,13S)-3,16-dihydroxyl-15-one-ent-pimar-8(14)-ene-3-O- β -D-glucopyranoside (**11**)

Colorless gum; $[\alpha]_{\text{D}}^{25}$ −6.5 (c 0.23, MeOH); UV (MeOH) λ_{\max} ($\log \epsilon$) 204 (3.42) nm; CD (MeCN) (7.5×10^{-5} M) λ_{\max} ($\Delta \epsilon$) 218 (−1.00), 293 (+0.33) nm; IR (microscope) ν_{\max} 3352, 2936, 1709, 1363, 1074, 1016 and 655 cm^{-1} ; for ^1H and ^{13}C NMR spectroscopic data, see Tables 1 and 2; HRESIMS m/z 505.2760 $[\text{M}+\text{Na}]^+$ (calcd for $\text{C}_{26}\text{H}_{42}\text{O}_8\text{Na}$, 505.2772).

4.3.9. Lonchophylloid B (**10**)

Colorless needles ($\text{CHCl}_3/\text{petroleum ether}$); $[\alpha]_{\text{D}}^{25}$ −10.2 (c 0.13, MeOH); CD (MeCN) (9.4×10^{-5} M) λ_{\max} ($\Delta \epsilon$) 216 (−1.19), 291 (+0.31) nm; ESIMS m/z 343.3 $[\text{M}+\text{Na}]^+$.

4.4. Preparation of the 2,3-dibenzoate (**1a**)

Benzoyl chloride (100 μL) was added to a stirred solution of **1** (4.5 mg) in pyridine (1 mL) under N_2 with the mixture stirred for

8 h at room temperature. After evaporating the solvent *in vacuo*, the resulting crude oil was subjected to flash silica gel CC (petroleum ether/EtOAc, 4:1) to afford **1a** ($\text{C}_{33}\text{H}_{38}\text{O}_6$, 5.2 mg), which was determined by NMR and MS spectra. CD (MeCN) (1.5×10^{-4} M) λ_{\max} ($\Delta \epsilon$) 237 (+12.0), 222 (−15.3), 205 (−10.0), 196 (+13.4) nm. ^1H NMR (CD_3OD , 400 MHz): δ_{H} 0.96 (3H, s, H-20), 1.03 (3H, s, H-19), 1.15 (3H, s, H-18), 1.19 (3H, s, H-17), 5.24 (1H, d, $J = 9.4$ Hz, H-3), 5.44 (1H, dd, $J = 4.3, 9.4, 11.8$ Hz, H-2), 5.46 (1H, br s, H-14), 2.40 (1H, m, H-6 α), 2.17 (3H, dd, $J = 4.1, 12.3$ Hz, H-1 α , H-12 β and H-7 β), 1.55 (1H, m, H-1 β), 1.18 (1H, m, H-12 α), 1.65 (1H, m, H-11 α), 1.46 (1H, m, H-11 β), 1.73 (1H, m, H-6 β), 1.52 (1H, m, H-6 α), 1.51 (1H, m, H-5), 1.97 (1H, t, $J = 8.6$ Hz, H-9), [7.90 (2H, dd, $J = 1.3, 8.3$ Hz), 7.82 (2H, dd, $J = 1.3, 8.3$ Hz), 7.49 (2H, m), 7.35 (4H, m), 2,3-O-dibenzoate groups]. ^{13}C NMR (CD_3OD , 100 MHz): δ_{C} 179.2 (C-15), 139.5 (C-8), 127.8 (C-14), 82.7 (C-3), 72.0 (C-2), 55.1 (C-5), 51.6 (C-9), 44.4 (C-13), 43.6 (C-1), 41.0 (C-4), 40.6 (C-10), 36.4 (C-7), 34.5 (C-12), 29.4 (C-18), 28.0 (C-17), 23.3 (C-6), 21.4 (C-11), 18.6 (C-19), 15.7 (C-20), [(168.1, 134.4, 131.4, 130.6, 130.6, 129.7, 129.7) and (167.6, 134.3, 131.3, 130.6, 130.6, 129.5, 129.5), 2,3-O-benzoate groups]. ESIMS m/z 553.3 $[\text{M}+\text{Na}]^+$, 529.3 $[\text{M}-\text{H}]^-$.

4.5. Preparation of (S)- and (R)-MTPA esters of **2**

A solution of compound **2** (1.0 mg) in deuterated pyridine- d_5 (0.5 mL) was treated with (R)-MTPA chloride (10 μL) under N_2 in an NMR tube and immediately shaken until uniformly mixed. The mixture was stirred at room temperature for 8 h. The ^1H NMR spectrum, recorded directly from the reaction NMR tube, showed the production of the corresponding (S)-MTPA ester (**2a**). Preparation of (R)-MTPA ester (**2b**) was performed in the same manner by treatment of **2** (1.0 mg) with (S)-MTPA chloride.

4.5.1. (S)-MTPA ester (**2a**)

^1H NMR ($\text{C}_5\text{D}_5\text{N}$, 400 MHz): δ_{H} 7.60–7.41 (5H, m, phenyl of MTPA), 5.36 (1H, s, H-14), 4.92 (1H, $J = 6.2, 10.0$ Hz, H-3), 3.52 (3H, s, −OMe of MTPA), 1.28 (3H, s, H-17), 1.17 (3H, s, H-18), 0.92 (3H, s, H-19), 0.84 (3H, s, H-20), 2.42 (1H, m, H-7 α), 2.17 (2H, m, H-7 β and H-12 β), 1.88 (1H, m, H-2 α), 1.82 (1H, m, H-1 α), 1.73 (1H, m, H-9), 1.65 (2H, m, H-6 β and H-11 β), 1.54 (1H, m, H-2 β), 1.47 (2H, m, H-6 α and H-11 α), 1.45 (1H, m, H-1 β), 1.09 (1H, m, H-12 α), 1.06 (1H, m, H-5). HRESIMS m/z 545.2497 $[\text{M}+\text{Na}]^+$ (calcd for $\text{C}_{29}\text{H}_{37}\text{F}_3\text{O}_5\text{Na}$, 545.2491).

4.5.2. (R)-MTPA ester (**2b**)

^1H NMR ($\text{C}_5\text{D}_5\text{N}$, 400 MHz): δ_{H} 7.62–7.41 (5H, m, phenyl of MTPA), 5.36 (1H, s, H-14), 4.92 (1H, $J = 6.2, 10.0$ Hz, H-3), 3.65 (3H, s, −OMe of MTPA), 1.28 (3H, s, H-17), 1.21 (3H, s, H-18), 0.99 (3H, s, H-19), 0.83 (3H, s, H-20), 2.41 (1H, m, H-7 α), 2.15 (2H, m, H-7 β and H-12 β), 1.81 (1H, m, H-2 α), 1.77 (1H, m, H-1 α), 1.72 (1H, m, H-9), 1.66 (2H, m, H-6 β and H-11 β), 1.51 (1H, m, H-2 β), 1.47 (2H, m, H-6 α and H-11 α), 1.43 (1H, m, H-1 β), 1.08 (1H, m, H-12 α), 1.04 (1H, m, H-5). HRESIMS m/z 545.2501 $[\text{M}+\text{Na}]^+$ (calcd for $\text{C}_{29}\text{H}_{37}\text{F}_3\text{O}_5\text{Na}$, 545.2491).

4.6. Alkaline hydrolysis of **3**, **4** and **7**

A solution of each diterpenoid (2 mg) in (MeOH/ H_2O , 1 mL, 1:1) was stirred with aqueous NaOH (0.1 M, 0.5 mL) for 4 h at room temperature. The mixture was then treated with HCl (0.1 M) until pH 6–7 and subjected to Sephadex LH-20 using MeOH as eluent to afford the pure corresponding hydrolysis product, which was identified on the basis of its ^1H NMR spectrum, R_f values and specific rotation.

4.7. Determination of absolute configuration of the diol unit in **6** by Sznatzke's method

According to the reported literature procedure, a solution of diol (0.5 mg) in anhydrous DMSO (1 mL) was mixed with dimolybdenum tetraacetate (1.0 mg). The first CD of the mixture (ca. molar ratio 1:1.2 diol/dimolybdenum tetraacetate) was measured immediately after mixing, and its time evolution was monitored until stationary phase (about 10 min after mixing). The inherent CD was subtracted. The observed sign of the diagnostic band corresponding to the O–C–C–O dihedral angle at around 300 nm in the induced CD spectrum was correlated to the absolute configuration of the secondary alcohol.

4.8. Acid hydrolysis of **11** and determination of sugar configuration

Compound **11** (2 mg) was dissolved in 2 mL of 2 M HCl (*p*-dioxane/H₂O, 1:1) and heated until 100 °C and then reflux began, this being maintained for 4 h. After removing the dioxane *in vacuo*, the solution was then diluted with H₂O and extracted with CH₂Cl₂ (3 × 1 mL). The aqueous layer was evaporated *in vacuo* to obtain a neutral residue, which was analyzed by silica gel TLC (acetone/*n*-BuOH/H₂O, 6:3:1) together with an authentic sugar standard (glucose, *R_f* = 0.49). The remaining residue was dissolved in pyridine (200 μL), to which L-cysteine methyl ester hydrochloride (2 mg) was added. The mixture was stirred at 60 °C for 1 h; then *o*-tolyl isothiocyanate (20 μL) was added, and the mixture was stirred at 60 °C for another 1 h. The reaction mixture was directly analyzed by standard C₁₈ HPLC [a YMC-pack ODS-A column (250 × 10 mm, 5–5 mm, 12 nm), CH₃CN/H₂O, 25:75, 3 mL/min]. The peak (*t_R* = 19.0 min) coincided with a derivative of D-glucose, as compared with authentic D-glucose treated in the same way with *t_R* at 19.1 min.

4.9. NF-κB activity

4.9.1. Cell culture and viability assay

RAW264.7 cells, transfected with pNF-κB-Luc reporter plasmid, were used for determination of NF-κB activity and cell viability, as previously described (Xu et al., 2013). Briefly, cells were cultured in DMEM, supplemented with 10% FBS, penicillin (100 U/mL), streptomycin (100 μg/mL) and 500 μg/mL geneticin under a humidified 5% CO₂ and 95% air atmosphere at 37 °C for 24 h. Potential differences in cell viability were detected by pretreating the cells with different concentrations of samples for 24 h. After that, supernatants were removed, MTT (5 mg/mL in serum-free medium) was added, the cells were cultured for additional 4 h at 37 °C. Finally, the MTT medium was removed, DMSO (100 μL) was added, and the optical density was measured at 490 nm with an automated microplate reader.

4.9.2. Luciferase assay

RAW264.7/NF-κB-Luc cells were pretreated with different concentrations of samples (0.78, 1.56, 3.12, 6.25, 12.5, 25 and 50 μM) for 1 h prior to being stimulated with LPS (2 mg/mL, *Escherichia coli* 055:B5) for further incubation in the cell culture medium. After 6 h, the medium was removed and cold-PBS (150 μL) was added to wash each well. The cold-PBS was removed, cells were lysed with cell culture lysis reagent for 10 min on ice, and then the cell lysis solution was added to 96-well white opaque plates and mixed with the same volume of luciferase assay system reagent. Finally, the value of luminescence (LUM) in each well was measured by an automated microplate reader with 250 ms of the integration time. The luciferase activity was evaluated with the following equation: %inhibition = (1 – (LUM_{LPS} – LUM_{sample})/(LUM_{LPS} – LUM_{blank})) × 100. Where LUM_{LPS} is the value of the cells stimulated

with LPS, LUM_{sample} is the value of a tested sample and LUM_{blank} is the value of the cell without LPS stimulation. Nonlinear regression (with sigmoidal dose response) was used to calculate the IC₅₀ values using GraphPad Prism (GraphPad Software, Inc.). The values were expressed as means ± standard deviation (SD) for triplicate experiments.

Acknowledgements

This work was financially supported by Grants from the National Natural Science Foundation of China (No. 81102782), the Industry-University-Research Cooperation Program from Science and Technology Department of Guangdong Province (2013B090200059) and the Priming Scientific Research Foundation for the Junior Teacher of Medicine in Sun Yat-sen University.

Appendix A. Supplementary data

Supplementary data associated with this article can be found in the online version, at <http://dx.doi.org/10.1016/j.phytochem.2015.07.005>.

References

- Allouche, N., Apel, C., Martin, M.T., Dumontet, V., Guéritte, F., Litaudon, M., 2009. Cytotoxic sesquiterpenoids from Winteraceae of Caledonian rainforest. *Phytochemistry* 70, 546–553.
- Bai, J., Chen, H., Fang, Z.F., Yu, S.S., Wang, W.J., Liu, Y., Ma, S.G., Li, Y., Qu, J., Xu, S., Liu, J.H., Liu, J.H., Zhao, F., Zhao, N., 2012. Sesquiterpenes from the roots of *Illicium dunnianum*. *Phytochemistry* 80, 137–147.
- Chen, J.L., Zhao, Z.M., Xue, X., Tang, G.H., Zhu, L.P., Yang, D.P., Jiang, L., 2014a. Bioactive norditerpenoids from *Flickingeria fimbriata*. *RSC Adv.* 4, 14447–14456.
- Chen, J.L., Zhong, W.J., Tang, G.H., Li, J., Zhao, Z.M., Yang, D.P., Jiang, L., 2014b. Norditerpenoids from *Flickingeria fimbriata* and their inhibitory activities on nitric oxide and tumor necrosis factor-α production in mouse macrophages. *Molecules* 19, 5863–5875.
- Costantino, V., Fattorusso, E., Mangoni, A., Perinu, C., Cirino, G., De Gruttola, L., Roviezzo, F., 2009. Tedanol: a potent anti-inflammatory ent-pimarane diterpene from the Caribbean Sponge *Tedania ignis*. *Bioorg. Med. Chem.* 17, 7542–7547.
- Di Bari, L., Pescitelli, G., Pratelli, C., Pini, D., Salvadori, P., 2001. Determination of absolute configuration of acyclic 1,2-diols with Mo₂(OAc)₄.1. Sznatzke's method revisited. *J. Org. Chem.* 66, 4819–4825.
- Didonato, J.A., Mercurio, F., Karin, M., 2012. NF-κB and the link between inflammation and cancer. *Immunol. Rev.* 246, 379–400.
- Frelek, J., Geiger, M., Voelter, W., 1999. Transition metal complexes as auxiliary chromophores in chiroptical studies on carbohydrates. *Curr. Org. Chem.* 3, 117–146.
- Harada, N., Nakanishi, K., 1972. The exciton chirality method and its application to configurational and conformational studies of natural products. *Acc. Chem. Res.* 5, 257–263.
- Jakupovic, J., Castro, V., Bohlmann, F., 1987. Millerenolides, sesquiterpene lactones from *Milleria quinqueflora*. *Phytochemistry* 26, 2011–2017.
- Lawrence, T., Gilroy, D.W., Colville-Nash, P.R., Willoughby, D.A., 2001. Possible new role for NF-κB in the resolution of inflammation. *Nat. Med.* 7, 1291–1297.
- Liu, H., Li, F., Li, C.J., Yang, J.Z., Li, L., Chen, N.H., Zhang, D.M., 2014. Bioactive furanocoumarins from stems of *Clausena lansium*. *Phytochemistry* 107, 141–147.
- Liu, X.F., Shen, Y., Yang, F., Hamann, M.T., Jiao, W.H., Zhang, H.J., Chen, W.S., Lin, H.W., 2012. Simplexolides A–E and plakorfuran A, six butyrate derived polyketides from the marine sponge *Plakortis simplex*. *Tetrahedron* 68, 4635–4640.
- Ma, G.X., Wang, T.S., Yin, L., Pan, Y., Guo, Y.H., LeBlanc, G.A., Reinecke, M.G., Watson, W.H., Krawiec, M., 1998. Two pimarane diterpenoids from *Ephemerantha lonchophylla* and their evaluation as modulators of the multidrug resistance phenotype. *J. Nat. Prod.* 61, 112–115.
- Moon, K.Y., Hahn, B.S., Lee, J., Kim, Y.S., 2001. A cell-based assay system for monitoring NF-κB activity in human HaCaT transfectant cells. *Anal. Biochem.* 292, 17–21.
- Ohtani, I., Kusumi, T., Kashman, Y., Kakisawa, H., 1991. High-field FT NMR application of Mosher's method. The absolute configurations of marine terpenoids. *J. Am. Chem. Soc.* 113, 4092–4096.
- Possebom, M.I., Mizokami, S.S., Carvalho, T.T., Zarpelon, A.C., Hohmann, M.S.N., Staurengo-Ferrari, L., Ferraz, C.R., Hayashida, T.H., De Souza, A.R., Ambrosio, S.R., Arakawa, N.S., Casagrande, R., Verri, W.A., 2014. Pimaradienoic acid inhibits inflammatory pain: Inhibition of NF-κB activation and cytokine production and activation of the NO-cyclic GMP-protein kinase G-ATP-sensitive potassium channel signaling pathway. *J. Nat. Prod.* 77, 2488–2496.

- Rothwarf, D.M., Karin, M., 1999. The NF-kappa B activation pathway: a paradigm in information transfer from membrane to nucleus. *Science* 5, 1–16.
- Snatzke, G., Wagner, U., Wolff, H.P., 1981. Circular dichroism of Cotton-type derivatives of chiral bidentate ligands with the complex [Mo₂(OOCCH₃)₄]. *Tetrahedron* 37, 349–361.
- Song, L.R., 1999. *Chinese Materia Medica (Zhonghua BenCao)*. Springer, Shanghai, vol. 8, pp. 711–712.
- Tanaka, T., Nakashima, T., Ueda, T., Tomii, K., Kouno, I., 2007. Facile discrimination of aldose enantiomers by reversed-phase HPLC. *Chem. Pharm. Bull.* 55, 899–901.
- Tornatore, L., Thotakura, A.K., Bennett, J., Moretti, M., Franzoso, G., 2012. The nuclear factor kappa B signaling pathway: integrating metabolism with inflammation. *Trends Cell Biol.* 22, 557–566.
- Wang, C., Li, C.J., Yang, J.Z., Ma, J., Chen, X.G., Hou, Q., Zhang, D.M., 2013a. Anti-inflammatory sesquiterpene derivatives from the leaves of *Tripterygium wilfordii*. *J. Nat. Prod.* 76, 85–90.
- Wang, G.C., Li, G.Q., Geng, H.W., Li, T., Xu, J.J., Ma, F., Wu, X., Ye, W.C., Li, Y.L., 2013b. Eudesmane-type sesquiterpene derivatives from *Laggera alata*. *Phytochemistry* 96, 201–207.
- Wang, R., Chen, W.H., Shi, Y.P., 2010. *Ent*-Kaurane and *ent*-pimarane diterpenoids from *Siegesbeckia pubescens*. *J. Nat. Prod.* 73, 17–21.
- Wu, Z.Y., Zhang, Y.B., Zhu, K.K., Luo, C., Zhang, J.X., Cheng, C.R., Feng, R.H., Yang, W.Z., Zeng, F., Wang, Y., Xu, P.P., Guo, J.J., Liu, X., Guan, S.H., Guo, D.A., 2014. Anti-inflammatory diterpenoids from the root bark of *Acanthopanax gracilistylus*. *J. Nat. Prod.* 77, 2342–2351.
- Xu, J., Jia, Y.Y., Chen, S.R., Ye, J.T., Bu, X.Z., Hu, Y., Ma, Y.Z., Guo, J.L., Liu, P.Q., 2013. (E)-1-(4-ethoxyphenyl)-3-(4-nitrophenyl)-prop-2-en-1-ol suppresses LPS induced inflammatory response through inhibition of NF- κ B signaling pathway. *Int. Immunopharmacol.* 15, 743–751.
- Zhang, Y., Wang, J.S., Luo, J., Kong, L.L., 2011. Novel nortriterpenoids from *Aphanamixis grandifolia*. *Chem. Pharm. Bull.* 59, 282–286.